Polymer 50 (2009) 5333–5340

Contents lists available at ScienceDirect

Polymer

journal homepage: www.elsevier.com/locate/polymer

Dissipative particle dynamics study on the multicompartment micelles self-assembled from the mixture of diblock copolymer poly(ethyl ethylene)-*block*-poly(ethylene oxide) and homopolymer poly(propylene oxide) in aqueous solution

Ying Zhao, Li-Yan You, Zhong-Yuan Lu*, Chia-Chung Sun

State Key Laboratory of Theoretical and Computational Chemistry, Institute of Theoretical Chemistry, Jilin University, Liu Tiao Road 2#, Changchun 130023, China

ARTICLE INFO

Article history:
Received 6 June 2009
Accepted 6 September 2009
Available online 11 September 2009

Keywords:
Multicompartment micelles
Dissipative particle dynamics simulation
Dilute solution

ABSTRACT

Dissipative particle dynamics (DPD) method is applied to model the self-assembly of diblock copolymer poly(ethyl ethylene)-*block*-poly(ethylene oxide) (PEE-*b*-PEO) and homopolymer poly(propylene oxide) (PPO) in aqueous solution. In this study, several segments are coarse-grained into a single simulation bead based on the experimental density. For the self-assembly of pure diblock copolymer PEE-*b*-PEO in dilute solution, the DPD simulation results are in good agreement with experimental data of micelle morphologies and sizes. The chain lengths of the block copolymers and the volume ratios between PPO and PEE-*b*-PEO are varied to find the conditions of forming multicompartment micelles. The micelles with core–shell–corona structure and the micelles with two compartments are both formed from the mixture of PEE-*b*-PEO and PPO in aqueous solution.

1. Introduction

As new and advanced nanomaterials, multicompartment micelles attract researchers in both academic and application fields due to their potential applications in biomedicine, drug delivery, and biotechnology [1,2]. The concept of multicompartment micelles was firstly proposed by Ringsdorf in order to mimic basic behaviors of natural systems such as serum albumin, which are not only responsible for the transport of poorly water-soluble compounds in the blood, but also uptake and release of different "transport goods" selectively [1]. Multicompartment micelles possess a hydrophilic shell and one to several compartments in a hydrophobic core, which can perform an array of distinct functions. Although such an innovative concept is very appealing, the precise preparation and control of stable multicompartment micelles are still at the start.

In the past few years, diverse approaches based on triblock copolymers for preparing multicompartment micelles had been developed by several groups [1–15], since diblock copolymers can only be divided into "core" and "corona" domains. Some progresses to self-assemble several discrete subdomains within one hydrophobic core had already been made with linear triblock copolymers [11–15]. For example, Laschewsky and co-workers found the "spheres on spheres" multicompartment micelles prepared by the self-assembly of linear ABC triblock copolymers poly(4-methyl-4-(4-vinylbenzyl)morpholin-4-ium chloride)-*block*-polystyrene-*block*-poly(pentafluorophenyl 4-vinylbenzyl ether)(PVBM-*b*-PS-*b*-PVBFP) in aqueous medium [11]. Thünemann et al. observed two-sphere and cylindrical multicompartment micelles formed from linear ABCBA pentablock copolymer in dilute aqueous solution [12]. Since the pioneer work by Lodge and co-workers [3], most investigations had been focused on the structure and morphology of multicompartment micelles formed from star triblock copolymers. They synthesized a series of ABC miktoarm star triblock copolymers μ-[poly(ethyl ethylene)][poly(ethylene oxide)][poly(perfluoropropylene oxide)] (μ-EOF) in dilute aqueous solution, and visualized clearly two separated compartments in a single micelle [3]. They further demonstrated that two incompatible agents could be separately or simultaneously stored in the discrete subdomains of the multicompartment micelles [4].

For multicompartment micelles to be most effective in applications, their sizes, shapes, and chemical structures must be controlled precisely. A promising strategy to tune the multicompartment micelle structures is by mixing different types of polymer components. Li et al. obtained a unique "hamburger" multicompartment micelle, from a binary mixture of spherical micelles, formed from EO diblock copolymers, and segmented worm-like micelles, formed from μ-EOF miktoarm star terpolymers [5]. Exciting examples for the preparation of stable multicompartment micellar systems have been

* Corresponding author.
E-mail address: luzhy@mail.jlu.edu.cn (Z.-Y. Lu).

0032-3861/$ – see front matter © 2009 Elsevier Ltd. All rights reserved.
doi:10.1016/j.polymer.2009.09.014

realized, but the hitherto employed synthetic methods are complicated. Therefore, more simple and economical approaches to form multicompartment micelles are requested. In this work, we investigate the formation of multicompartment micelles from the mixture of diblock copolymer poly(ethyl ethylene)-*block*-poly(ethylene oxide) (PEE-*b*-PEO) and homopolymer poly(propylene oxide) (PPO) in dilute aqueous solution by dissipative particle dynamics (DPD) simulations, which had been illustrated to be a powerful tool for better understanding the self-assembly mechanism of the multicompartment micelles [16–23]. In this study, several polymer segments are systematically coarse-grained into a single simulation bead based on the experimental density. Different beads are assumed to have equal volume, and the interaction parameters between beads are estimated from Flory–Huggins χ parameters, obtained either from available experiments or from atomistic molecular dynamics simulations.

2. Mesoscale simulation method and coarse-grain mapping

2.1. Mesoscale simulation method: dissipative particle dynamics

DPD is a mesoscopic simulation technique introduced by Hoogerbrugge and Koelman in 1992 [24]. A DPD bead represents a group of atoms or a volume of fluid that is large on the atomistic scale but still macroscopically small [25]. The force experienced by particle i is composed of three parts: a conservative force $\mathbf{F}^C$, a dissipative force $\mathbf{F}^D$, and a random force $\mathbf{F}^R$. To model the block copolymers, we tie the adjacent beads in a single polymer chain by harmonic spring force $\mathbf{F}^S$. Each force is pairwise additive:

$$\mathbf{F}_i = \sum_{j\neq i}(\mathbf{F}_{ij}^C + \mathbf{F}_{ij}^D + \mathbf{F}_{ij}^R + \mathbf{F}_{ij}^S). \tag{1}$$

The sum runs over all other particles within a certain cutoff radius R_c. The different parts of the forces are given by:

$$\mathbf{F}_{ij}^C = -\alpha_{ij}\omega^C(r_{ij})\mathbf{e}_{ij}, \tag{2}$$

$$\mathbf{F}_{ij}^D = -\gamma\omega^D(r_{ij})(\mathbf{v}_{ij}\cdot\mathbf{e}_{ij})\mathbf{e}_{ij}, \tag{3}$$

$$\mathbf{F}_{ij}^R = \sigma\omega^R(\mathbf{r}_{ij})\xi_{ij}\Delta t^{-1/2}\mathbf{e}_{ij}, \tag{4}$$

where $\mathbf{r}_{ij}=\mathbf{r}_i-\mathbf{r}_j$, $r_{ij}=|\mathbf{r}_{ij}|$, $\mathbf{e}_{ij}=\mathbf{r}_{ij}/r_{ij}$, $\mathbf{r}_i$ and $\mathbf{r}_j$ are the positions of particle i and particle j, respectively. $\mathbf{v}_{ij}=\mathbf{v}_i-\mathbf{v}_j$, $\mathbf{v}_i$ and $\mathbf{v}_j$ are the velocities of particle i and particle j, respectively. α_{ij} is a constant which describes the maximum repulsion between interacting beads. γ and σ are the amplitudes of dissipative and random forces, respectively. ω^C, ω^D, and ω^R are three weight functions for the conservative, dissipative, and random forces, respectively. For the conservative force, we choose $\omega^C(r_{ij}) = 1 - r_{ij}/R_c$ for $r_{ij} < R_c$ and $\omega^C(r_{ij}) = 0$ for $r_{ij} \geq R_c$. $\omega^D(r_{ij})$ and $\omega^R(r_{ij})$ follow a certain relation according to the fluctuation–dissipation theorem [26],

$$\omega^D(r) = \left[\omega^R(r)\right]^2, \quad \sigma^2 = 2\gamma k_B T. \tag{5}$$

Here we choose a simple form of ω^D and ω^R following Groot and Warren [25],

$$\omega^D(r) = \left[\omega^R(r)\right]^2 = \begin{cases} (1-r/R_c)^2 & (r < R_c) \\ 0 & (r \geq R_c) \end{cases} \tag{6}$$

ξ_{ij} is a random number with zero mean and unit variance, chosen independently for each interacting pair of beads at each time step Δt. A modified version of velocity-Verlet algorithm [25,27] is used here to integrate the equations of motion. For easy numerical handling, we have chosen the cutoff radius, the particle mass, and the temperature as the units of the simulated system, i.e., $R_c = m = k_BT = 1$. As a consequence, the unit of time τ is $\tau = R_c\sqrt{m/k_BT} = 1$.

The conservative interaction strength α_{ij} is chosen according to the linear relation with Flory–Huggins χ parameters by

$$\alpha_{ij} \approx \alpha_{ii} + 3.497\chi_{ij} \quad (\rho = 3), \tag{7}$$

where the interaction parameter between the same type of bead α_{ii} equals 25 to correctly describe the compressibility of water [25], and $\rho = 3$ is the number density in our simulations. The spring force $\mathbf{F}_{ij}^S = Cr_{ij}$, and the spring constant C is set to be 4.0, which is enough to keep the adjacent beads connected together along the polymer backbone [27].

2.2. Coarse-grain mapping

To find more simple and economical approach of forming multicompartment micelles, we consider to mix diblock copolymer and homopolymer in water. PEE-*b*-PEO is a suitable choice as the diblock copolymer since it can self-assemble into various nanoaggregates in water [7]. The homopolymer should be hydrophobic and immiscible with PEE to form different cores of the multicompartment micelles. Thus, PPO may be the choice which cannot only satisfy the above criterion but also is nontoxic and economical. Therefore, we consider the system which contains water, diblock copolymer PEE-*b*-PEO and homopolymer PPO.

First of all, we need to determine the volume of the simulation beads in order to construct a mesoscopic model. Different beads that represent a number of monomers are assumed to have equal volume, which is necessary to conform to the Flory–Huggins theory and the standard DPD model [28–33]. The same density of the beads for all species is restricted to make stronger link with experiments [34]. According to the molecular weights and the bulk densities of the pure species in experiments [7], the volumes of the monomers can be obtained, as shown in Table 1.

In Ref. [7], the diblock copolymers PEE-*b*-PEO are designated by EO($x-y$), where x and y denote the molecular weights divided by 1000 of the PEE and PEO blocks, respectively. To coarse-grain map onto these experimental systems of EO($x-y$), we take 20 water molecules together and group them into one bead in our simulations. Therefore, the reference volume of one bead adds up to 600 Å^3, which approximately equals to the volume of 6 PEE monomers, or 9 PEO monomers, or 5 PPO monomers. Thus, the experimental systems of EO($x-y$) are coarse-grained and the corresponding simulation models are shown in Table 2.

The key parameters, characterizing the bead–bead interactions in DPD model, can be estimated from the Flory–Huggins χ parameters via Eq. (7). First, we try to look for the Flory–Huggins χ parameters in the literatures. Since PEO is miscible with water at almost any concentrations, the value $\chi(\text{PEO}-\text{water}) = 0.3$ is used here in agreement with the value obtained by Groot and Rabone for the two species [35], which is also adopted in other literatures [34,36]. In Refs. [36–38], they used $\chi(\text{PEO}-\text{PPO}) = 3.0$ estimated from group contribution method corresponding to the bead volume

Table 1
Molecular parameters in the system. The monomer volumes are calculated using the molecular weight and the experimental bulk densities at room temperature [7].

	Molecular weight M(g/mol)	Density ρ(g/cm^3)	Monomer volume V(Å^3)	Monomer number per DPD bead
Water	18	1.0	30	20
PEE	56	0.866	107	6
PEO	44	1.12	65	9
PPO	58	0.821	118	5

Table 2
The experimental samples EO($x-y$), where x and y denote the molecular weights divided by 1000 of PEE and PEO blocks, respectively, are coarse-grained to E_aO_b, where a and b denote the number of the PEE and PEO beads in the DPD simulations. f_{PEO} is the volume fraction of PEO in diblock copolymer. The hydrodynamic radius R_h can be measured by dynamic light scattering (DLS). The sizes of the micelles are calculated from the mean radius of gyration R_g and $R_{g,\,c}$ of the overall micelles and the micellar cores. S and C represent sphere and cylinder micelles, respectively.

Experiment [7]				Simulation		
Sample	f_{PEO}	R_h(nm)	Morphology	Coarse-gained	$R_g(R_{g,\,c})$(nm)	Morphology
EO(1.4–2)	0.52	21	S + C	E_4O_4		C
EO(1.4–5)	0.74	19	S	E_4O_{11}	4.4(2.3)	S
EO(2–4)	0.59	23	S + C	E_5O_8	4.8(3.1)	S + C
EO(2–6)	0.69	23	S	E_5O_{13}	4.8(2.5)	S
EO(2–7)	0.72	23	S	E_5O_{15}	4.8(2.3)	S
EO(2–9)	0.78	24	S	E_5O_{20}	5.1(2.1)	S

of 150 Å^3. Hence, the Flory–Huggins interaction parameter $\chi(\mathrm{PEO}-\mathrm{PPO}) = 12.0$ is estimated here in accordance to the bead volume of 600 Å^3 in our simulations. Similarly, $\chi(\mathrm{PPO}-\mathrm{water}) = 8.4$ corresponding to the bead volume of 600 Å^3 is also deduced from the published data [36].

The Flory–Huggins χ parameters for PEE–PEO, PEE–PPO, and PEE–water at $T = 298$ K are not found in the literatures. In fact, the χ parameters for polymer beads (PEE–PEO and PEE–PPO) can be calculated from the solubility parameters of the pure species [39], which are obtained from molecular dynamics (MD) simulations in this research. Each chain of PEE, PEO, and PPO possesses roughly the same volume (600 Å^3) in our MD simulations, where PEE consists of 6 monomers per chain, PEO 9 monomers per chain, and PPO 5 monomers per chain. This method that the volume of each polymer chain is the same is consistent with that in Ref. [40]. In the simulations, the PEE, PEO, and PPO chains are firstly constructed in a side length $L = 18$ Å box with 3-D periodic boundary conditions at the experimental densities, respectively. A high-quality force field COMPASS (condensed-phase optimized molecular potentials for atomistic simulation studies) [41–43] is adopted, which is known to accurately reproduce experimental structures, densities, and solubility parameters [39]. The Coulomb interactions are calculated via Ewald summation [44,45]. In the beginning of the simulations, energy minimizations are performed to relax the local unfavorable structures of the chains. Subsequently, 1000 ps MD simulations are performed under *NPT* thermodynamic ensemble with integration time steps 1 fs. Each simulation is performed for six times with different initial configurations to ensure the reliability of the results. Constant temperature $T = 298$ K and pressure $P = 0.1$ GPa are controlled through the Berendsen thermostat and barostat [46].

In our MD simulations, we can obtain the cohesive energy E_{coh} by [47]

$$E_{\mathrm{coh}} = \left(\sum_{i=1}^{n} E_{nb}^{\mathrm{isolated}}(i) - E_{nb}^{n}\right) \Big/ n, \tag{8}$$

where $E_{nb}^{\mathrm{isolated}}(i)$ is the nonbonded energy for the ith isolated chain in vacuum, and E_{nb}^{n} the nonbonded energy of the model with n chains in periodic boundary conditions. The solubility parameter δ is the square root of the cohesive energy density [39],

$$\delta = \sqrt{E_{\mathrm{coh}}/V}, \tag{9}$$

where V is the volume of the box at equilibrium. The Flory–Huggins χ parameter can be calculated from the solubility parameters by the equation [48]

$$\chi_{12} = \frac{V_{\mathrm{bead}}}{k_{\mathrm{B}}T}(\delta_1 - \delta_2)^2, \tag{10}$$

where V_{bead} is the volume of the bead size in DPD. Therefore, we can obtain the solubility parameters from MD simulations, $\delta(\mathrm{PEO}) = 20.74$ (J/cm^3)$^{1/2}$, $\delta(\mathrm{PEE}) = 16.41$ (J/cm^3)$^{1/2}$, and $\delta(\mathrm{PPO}) = 19.49$ (J/cm^3)$^{1/2}$, subsequently estimate the Flory–Huggins interaction parameters between DPD beads $\chi(\mathrm{PEE}-\mathrm{PEO}) = 2.74$ and $\chi(\mathrm{PEE}-\mathrm{PPO}) = 1.38$.

For a dilute solution, the volume fractions of water and polymer are very different. In this case we have to adopt the following equations [40]:

$$\chi = V_{\mathrm{bead}}\left(\frac{\Delta E_{\mathrm{mix}}}{k_{\mathrm{B}}T}\right), \tag{11}$$

$$\Delta E_{\mathrm{mix}} = \phi_A\left(\frac{E_{\mathrm{coh}}}{V}\right)_A + \phi_B\left(\frac{E_{\mathrm{coh}}}{V}\right)_B - \left(\frac{E_{\mathrm{coh}}}{V}\right)_{AB}, \tag{12}$$

to estimate the χ parameter between water and PEE. Here, ΔE_{mix} is the mixing energy. ϕ_A and ϕ_B are the volume fractions of the two components in the dilute solution. In this work, $\phi_{\mathrm{water}} \approx 1$ and $\phi_{\mathrm{PEE}} \approx 0$ are used. We calculate $(E_{\mathrm{coh}}/V)_{AB} = 2191.48$ J/cm^3 from MD simulations and then estimate $\chi(\mathrm{PEE}-\mathrm{water}) = 15.02$ using Eqs. (11) and (12). The Flory–Huggins χ parameters between different types of molecules are summarized in Table 3.

According to Eq. (7), the repulsion parameters α_{ij} between DPD beads are calculated from the Flory–Huggins χ parameters and shown in Table 4. Although DPD is a simple but intrinsically promising simulation method to study the multicompartment micelles, computational cost is still a limiting factor. Our DPD code is thus parallelized using a spatial domain decomposition method [49,50] with the aid of the standard message passing interface library. In our previous works [23,51], the parallel DPD code is verified to be accurate and possesses high efficiency. In this research, our parallel DPD simulations are performed in a cubic box of size $40 \times 40 \times 40R_c^3$ containing 1.92×10^5 beads. The concentration of the block copolymers is $\phi = 0.05$–0.10 to guarantee the dilute solution. Periodic boundary conditions are applied. The integration time step Δt is taken as 0.05, 2×10^5 DPD time steps are carried out for each system.

3. Results and discussion

In general, PEE-*b*-PEO dilute aqueous solution can be well equilibrated after about 1×10^5 time steps. To examine whether the simulations are completely equilibrated, the variation of mean aggregate number $\langle P\rangle$ with time is calculated. The mean aggregate number $\langle P\rangle$ can be expressed as $\langle P\rangle_n$, which is defined by $\langle P\rangle_n = \sum_i P_i n_i$, where n_i denotes the number fraction of the

Table 3
Molecule and molecule interaction parameters χ_{ij}.

	Water	PEE	PEO	PPO
Water	0.00			
PEE	15.02	0.00		
PEO	0.3	2.74	0.00	
PPO	8.4	1.38	12.0	0.00

Table 4
DPD bead–bead interaction parameters α_{ij}.

	Water	PEE	PEO	PPO
Water	25.00			
PEE	77.52	25.00		
PEO	26.05	34.58	25.00	
PPO	54.37	29.84	66.96	25.00

aggregate with aggregation number equals to P_i and $\sum_i n_i = 1$ [52]. As an example, the typical variation of the mean aggregate number $\langle P\rangle_n$ with time for E_5O_{15} system is shown in Fig. 1. $\langle P\rangle_n$ is determined every 2000 steps before 1×10^4 time steps and every 10,000 steps after 1×10^4 time steps. It can be seen that after 1×10^5 time steps, the value of $\langle P\rangle_n$ is almost constant, which clearly demonstrates that the system reaches equilibrium [52].

Fig. 2 shows the equilibrium morphologies corresponding to 2×10^5 time step simulations of PEE-*b*-PEO dilute solutions. Model E_4O_4 ($f_{PEO}=0.52$, f_{PEO} is the volume fraction of PEO in the diblock copolymer), which is in accordance to the experiment model EO(1.4–2) (cf. Table 2), forms cylindrical micelles as shown in Fig. 2(a) when the concentration of E_4O_4 is 0.05. Model E_5O_8 ($f_{PEO}=0.59$) in dilute solutions forms the mixtures of spherical and cylindrical micelles, E_4O_{11} ($f_{PEO}=0.74$), E_5O_{13} ($f_{PEO}=0.69$), E_5O_{15} ($f_{PEO}=0.72$), and E_5O_{20} ($f_{PEO}=0.78$) in dilute solutions can form spherical micelles, as shown in Fig. 2(b)–(f), respectively. These results are in good agreement with the experimental results [7].

To estimate the sizes of the micelles, the mean radius of gyration R_g of the micelles are calculated. The whole simulation box is firstly divided into many small equivalent cubic cells. Then according to the positions of the beads of the block copolymers, we can find whether there are block copolymers in each cubic cell. There must be no DPD beads belonging to the block copolymers in the cells which are located between different micelles, so we can find which block copolymer beads belong to the same micelles. Then, the number of the micelles is calculated. Finally, we calculate the radius of gyration of each micelle with the positions of block copolymer beads, and the mean radius of gyration of the micelles can also be obtained by averaging the radius of gyration of each micelle. Since the volume of one bead is 600 Å^3 and the number density is $\rho R_c^3=3$, a cube of R_c^3, therefore, corresponds to a volume of 1800 Å^3. Thus, natural length scale in the simulations can be obtained [35,53], $R_c=\sqrt[3]{1800}\ \text{Å}=1.22$ nm. Accordingly, the mean radius of gyration of the micelles (R_g) and the mean radius of gyration of the micellar cores ($R_{g,c}$) are shown in Table 2. For example, R_g and $R_{g,c}$ for the micelles formed by E_5O_{15} are 4.8 nm and 2.3 nm, respectively.

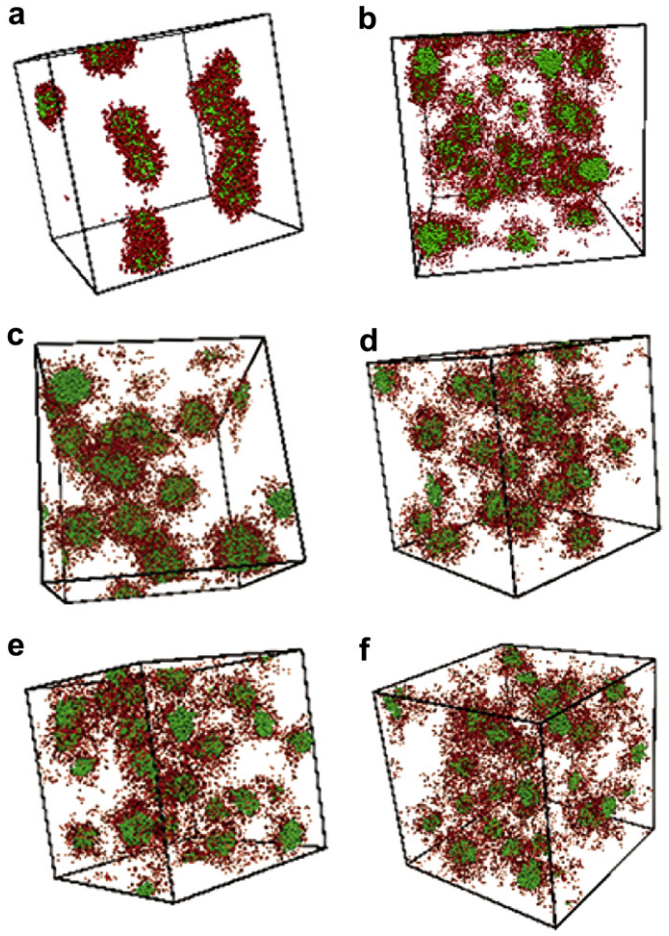

Fig. 2. The morphologies of PEE-*b*-PEO: (a) E_4O_4, (b) E_4O_{11}, (c) E_5O_8, (d) E_5O_{13}, (e) E_5O_{15}, and (f) E_5O_{20}. The volume fraction of the polymers (PEE-*b*-PEO) is always 0.10 to guarantee the dilute solution. Red particles represent hydrophilic PEO block, and green ones represent hydrophobic PEE block. (For interpretation of the references to colour in this figure legend, the reader is referred to the web version of this article.)

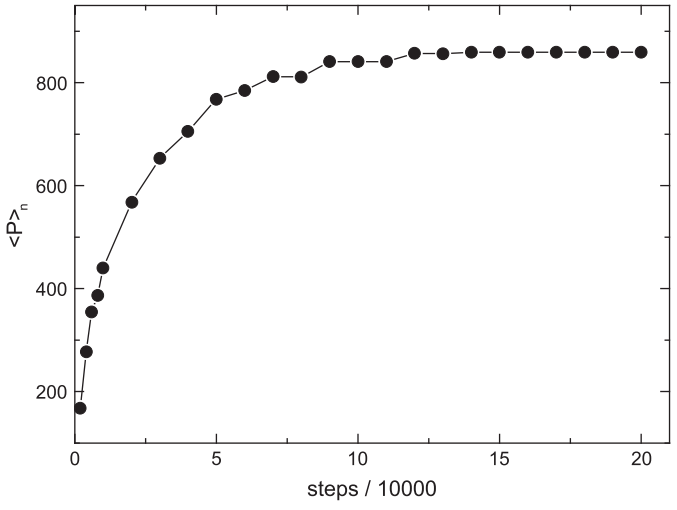

Fig. 1. The variation of mean aggregate number $\langle P\rangle_n$ with time for block copolymer E_5O_{15} solution. The mean aggregate number $\langle P\rangle_n$ is determined every 2000 steps before 1×10^4 time steps and every 10,000 steps after 1×10^4 time steps.

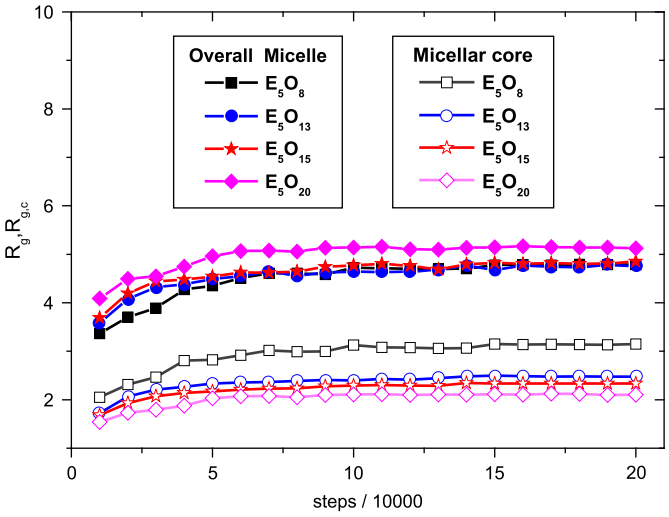

Fig. 3. The typical variation of the mean radius of gyration, R_g, of overall micelles and the mean radius of gyration, $R_{g,c}$, of the micellar cores with time for PEE-*b*-PEO.

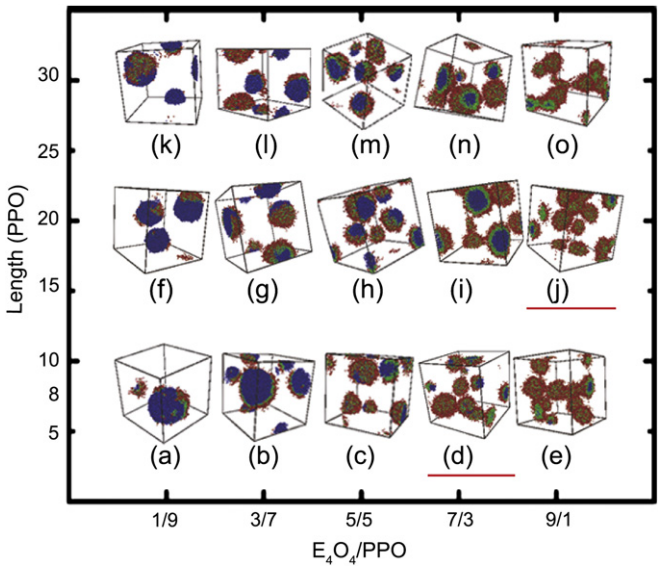

Fig. 4. The morphologies are obtained for E_4O_4/PPO system. The red particles represent PEO block, the green ones represent PEE block, and the blue ones represent PPO. The volume fraction ratios between E_4O_4 and PPO are 1:9, 3:7, 5:5, 7:3, and 9:1. The chain lengths of PPO are 8, 20, and 30, in which the chain length of 8 is equivalent with that of E_4O_4 block copolymer. The morphologies indicated by red lines are stable. (For interpretation of the references to colour in this figure legend, the reader is referred to the web version of this article.)

The time evolution of R_g and $R_{g,c}$ for PEE-*b*-PEO is shown in Fig. 3, in which the values of the mean radius of gyration are calculated every 1×10^4 time steps. It can be seen that the systems reach equilibrium after about 1×10^5 time steps, and R_g and $R_{g,c}$ reach plateau values. In experiments, the hydrodynamic radius R_h can be measured by dynamic light scattering (DLS). The DLS measures the radius of a hypothetical hard sphere with the diffusional properties under examination. In practice, hypothetical hard spheres are non-existent, and macromolecules in solution are non-spherical. So hydrodynamic radius R_h is much larger than the radius of gyration R_g of a micelle. In Table 2, we also show the experimental micelle sizes obtained by DLS. As demonstrated above, our results of micelle sizes are in qualitative agreement with those in experiments. Specially, we find that $R_g(E_4O_{11}) < R_g(E_5O_8) = R_g(E_5O_{13}) = R_g(E_5O_{15}) < R_g(E_5O_{20})$, which is in agreement with the size order in experiments. We also find that $R_{g,c}$ decreases with increasing hydrophilic PEO block length, i.e., $R_{g,c}(E_5O_8) > R_{g,c}(E_5O_{13}) > R_{g,c}(E_5O_{15}) > R_{g,c}(E_5O_{20})$. This is reasonable since when the ratio of hydrophilic PEO block increases, the longer PEO block means less number of PEE-*b*-PEO chains in the systems. Therefore, for the self-assembly of PEE-*b*-PEO in water, our simulation results are consistent with those from experiments [7], not only on the micelle morphologies but also on the micelle sizes, which indicate that our coarse-graining procedure and the DPD simulation method are appropriate for such a system.

Based on the coarse-graining and mesoscale simulation strategy, we then consider the self-assembly of the mixture of PEE-*b*-PEO and PPO in dilute aqueous solutions, and our main goal is to find the conditions of forming multicompartment micelles. The volume fraction of the total polymers (PEE-*b*-PEO and PPO) is kept at $\phi = 0.10$. To study the possibilities and conditions of forming multicompartment micelles, PPO of different chain length and PEE-*b*-PEO with different ratios are mixed in dilute aqueous solution.

Take E_4O_4/PPO_8 system as an example, here the subscript 8 means the chain length of PPO is 8. The morphologies after 2×10^5 time step

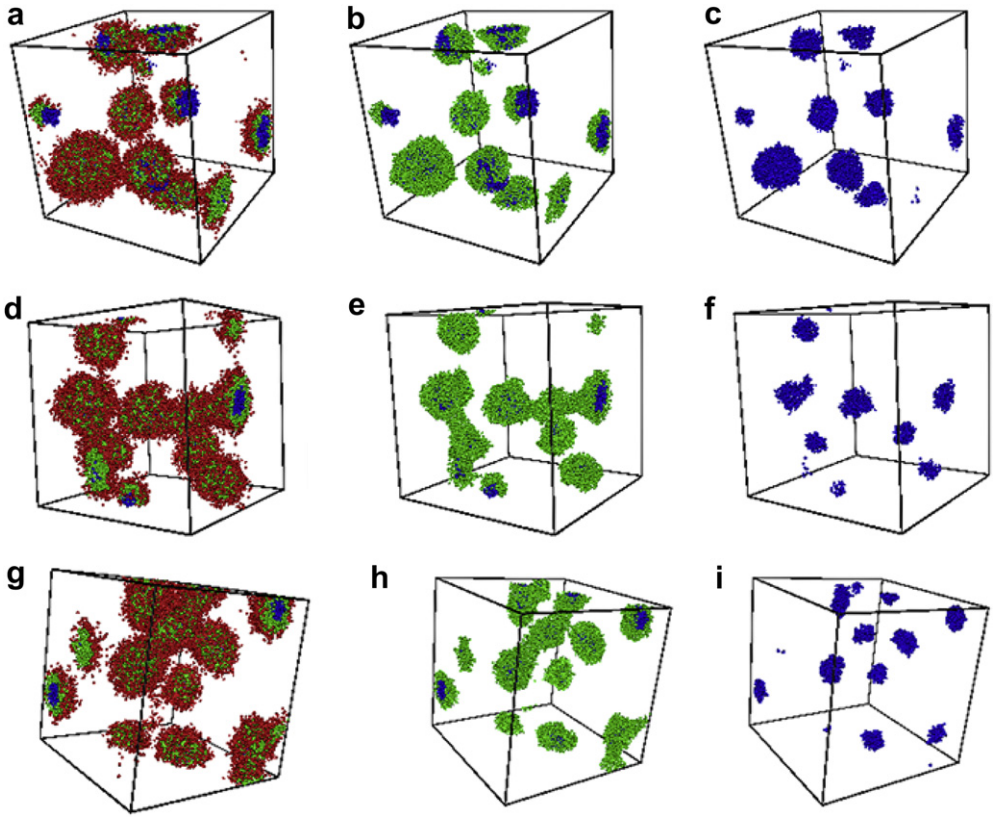

Fig. 5. The morphologies are obtained for E_4O_4/PPO_8 with $\gamma = 7:3$, $\gamma = 9:1$, and E_4O_4/PPO_{20} with $\gamma = 9:1$ systems. The red particles represent PEO block, the green ones represent PEE block, and the blue ones represent PPO. (a), (b), and (c) represent for the E_4O_4/PPO_8 with $\gamma = 7:3$; (d), (e), and (f) represent for the E_4O_4/PPO_8 with $\gamma = 9:1$; (g), (h), and (i) represent for the E_4O_4/PPO_{20} with $\gamma = 9:1$. (For interpretation of the references to colour in this figure legend, the reader is referred to the web version of this article.)

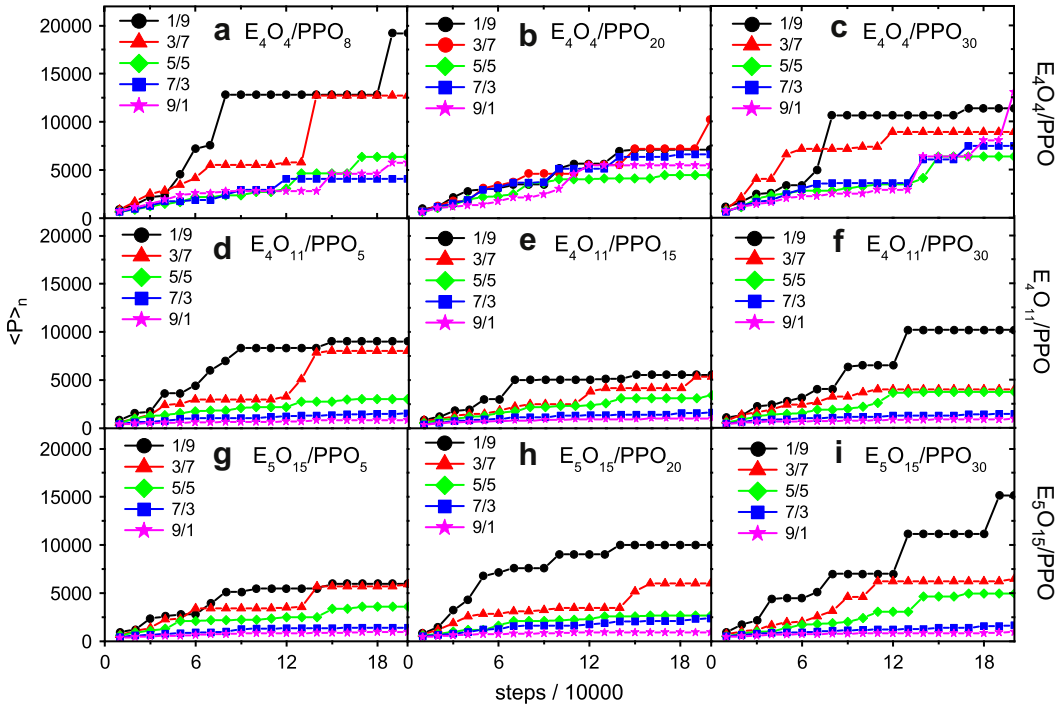

Fig. 6. The variation of mean aggregate number $\langle P\rangle_n$ with the time for E_xO_y/PPO system: (a) E_4O_4/PPO_8, (b) E_4O_4/PPO_{20}, (c) E_4O_4/PPO_{30}, (d) E_4O_{11}/PPO_5, (e) E_4O_{11}/PPO_{20}, (f) E_4O_{11}/PPO_{30}, (g) E_5O_{15}/PPO_5, (h) E_5O_{15}/PPO_{20}, (j) E_5O_{15}/PPO_{30}.

simulations with different compositions are summarized in Fig. 4. The volume fraction ratios (γ) between E_4O_4 and PPO_8 are 1:9, 3:7, 5:5, 7:3, and 9:1. The red particles represent the PEO block, the green ones represent the PEE block, and the blue ones represent PPO homopolymers. When $\gamma = 7{:}3$, the core–shell–corona (PPO–PEE–PEO) micelles are observed, as shown in Fig. 4(d). The volume fraction of the PPO_8 chains is less than that of E_4O_4 in this system, so the hydrophobic PPO domain can be wrapped by diblock copolymer E_4O_4 to avoid its contact to water. Although the PEE block is more hydrophobic than PPO, it is actually located between PPO and PEO domains because of the covalent bonds between PEE and PEO blocks. Thus, the micelle structure is core–shell–corona with PPO as the core, PEE the shell, and PEO the corona. To observe the inner structure of the multicompartment micelles clearly, the morphologies of E_4O_4/PPO_8 with $\gamma = 7{:}3$ are shown in Fig. 5(a)–(c). The time evolution of the mean aggregate number $\langle P\rangle_n$ for this system is also obtained, which demonstrates that after 2×10^5 time step simulation, the system reaches equilibrium completely as shown by the blue line[1] in Fig. 6(a).

For E_4O_4/PPO_8 with $\gamma = 9{:}1$, except for core–shell–corona micelles, we can also observe the multicompartment micelles with two PPO cores sharing one PEE shell as shown in Fig. 4(e). The inner structures of the multicompartment micelles are shown in Fig. 5(d)–(f). From the purple line[1] in Fig. 6(a) ($\langle P\rangle_n$), we find that for this system, the morphology obtained after 2×10^5 time step simulation is unstable. The time evolutions of the mean aggregate number $\langle P\rangle_n$ for E_4O_4/PPO_8 with $\gamma = 1{:}9$, $\gamma = 3{:}7$, and $\gamma = 5{:}5$ are also calculated to examine whether the simulations are equilibrated and shown in Fig. 6(a). The three systems are also unstable after 2×10^5 time step simulations. Especially, for E_4O_4/PPO_8 with $\gamma = 1{:}9$, we can observe only one PPO aggregate which is completely phase-separated from water.

To investigate the influence of the chain length of PPO on the formation of the multicompartment micelles, we change the chain length of PPO from 8 to 20 and 30, coarse-grained roughly from 40, 100, and 150 PO monomers, respectively. Increasing the chain length of PPO to 20, only the system with $\gamma = 9{:}1$ reaches equilibrium completely after 2×10^5 time step simulation (the purple line[1] in Fig. 6(b)). The mixture of core–shell–corona micelles and the micelle with three PPO cores sharing one PEE shell can be observed

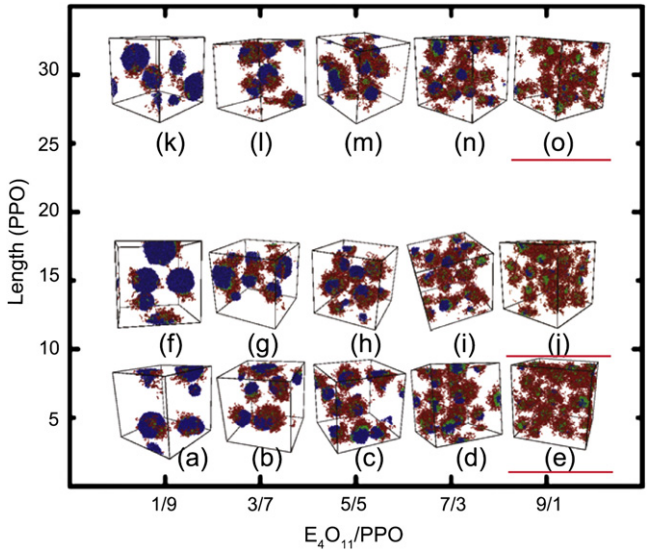

Fig. 7. The morphologies are obtained for E_4O_{11}/PPO system. The red particles represent PEO block, the green ones represent PEE block, and the blue ones represent PPO. The volume fraction ratios between E_4O_{11} and PPO are 1:9, 3:7, 5:5, 7:3, and 9:1. The chain lengths of PPO are 5, 15, and 30, in which the chain length of 15 is equivalent with that of E_4O_{11} block copolymer. The morphologies indicated by red lines are stable. (For interpretation of the references to colour in this figure legend, the reader is referred to the web version of this article.)

[1] (For interpretation of the references to colour in this figure legend, the reader is referred to the web version of this article.)

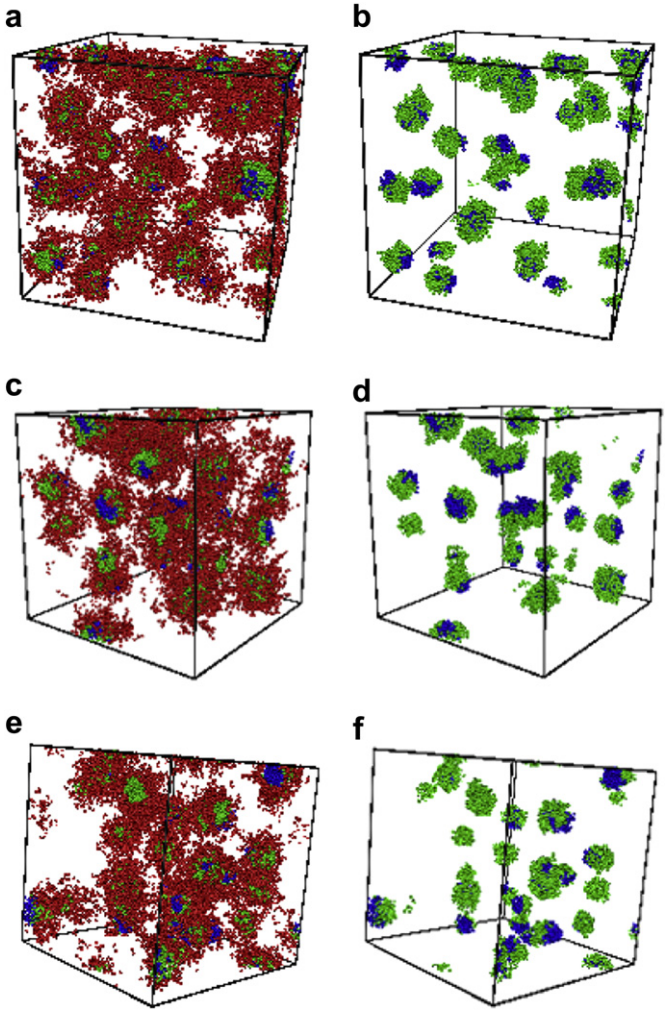

Fig. 8. The morphologies are obtained for E_4O_{11}/PPO_5 with $\gamma = 9{:}1$, E_4O_{11}/PPO_{15} with $\gamma = 9{:}1$, and E_4O_{11}/PPO_{20} with $\gamma = 9{:}1$ systems. The red particles represent PEO block, the green ones represent PEE block, and the blue ones represent PPO. (a), and (b) represent for the E_4O_{11}/PPO_5 with $\gamma = 9{:}1$; (c) and (d) represent for the E_4O_{11}/PPO_{15} with $\gamma = 9{:}1$; (e) and (f) represent for the E_4O_{11}/PPO_{20} with $\gamma = 9{:}1$. (For interpretation of the references to colour in this figure legend, the reader is referred to the web version of this article.)

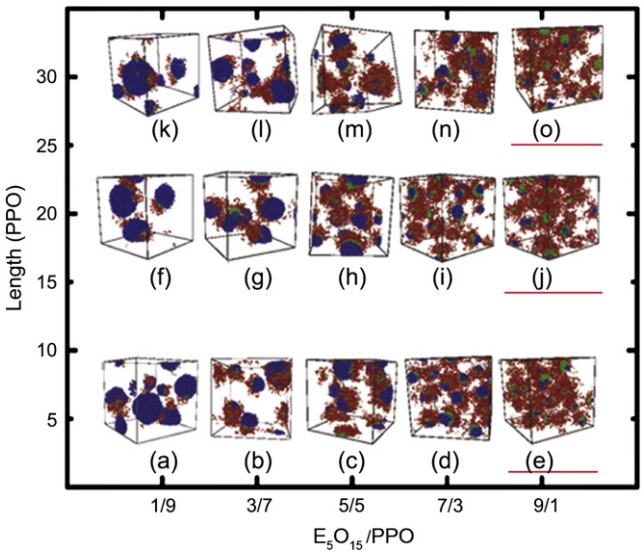

Fig. 9. The morphologies are obtained for E_5O_{15}/PPO system. The red particles represent PEO block, the green ones represent PEE block, and the blue ones represent PPO. The volume fraction ratios between E_5O_{15} and PPO are 1:9, 3:7, 5:5, 7:3, and 9:1. The chain lengths of PPO are 5, 20, and 30, in which the chain length of 20 is equivalent with that of E_5O_{15} block copolymer. The morphologies indicated by red lines are stable. (For interpretation of the references to colour in this figure legend, the reader is referred to the web version of this article.)

as shown in Fig. 5(g)–(i). When the chain length of PPO is 30, these systems with different compositions do not reach equilibrium after 2×10^5 time step simulation. Therefore, the mixture of core–shell–corona micelles and the micelle with two or three PPO cores sharing one PEE shell can be observed when the chain length of PPO is 8 at $\gamma = 7{:}3$ and 20 at $\gamma = 9{:}1$.

For E_4O_{11}/PPO system, the chain length of PPO is chosen as 5, 15, and 30, respectively. The self-assembly morphologies are shown in Fig. 7. The systems with $\gamma = 9{:}1$ reach equilibrium after 2×10^5 time step simulations, which can be demonstrated by the time evolution of the mean aggregate number $\langle P \rangle_n$ as shown in Fig. 6(d)–(f). Due to longer PEO block, the micelles with two independent spherical compartments (PPO and PEE) are formed as shown in Fig. 8. To investigate the influence of the chain length of PPO on the properties of the multicompartment micelles, the mean radius of gyration R_g of the overall micelles with $\gamma = 9{:}1$ are calculated. We obtain $R_g = 9.7$ nm with PPO chain length 5, $R_g = 4.7$ nm with PPO chain length 15, and $R_g = 8.5$ nm with PPO chain length 30. This result shows that when the chain length of PPO is shorter or longer than that of PEE-*b*-PEO, it is easy to form larger multicompartment micelles.

For E_5O_{15}/PPO system with $\gamma = 9{:}1$ and the chain length of PPO is chosen as 5, 20, and 30, the PEO block is long enough to totally protect all the PPO homopolymer and PEE block from contacting to water. Thus, the micelles with two spherical compartments (one is PPO and the other is PEE) are formed, as shown in Fig. 9(e), (j), and (o). Moreover, we also observe that the systems with $\gamma = 9{:}1$ reach equilibrium completely after 2×10^5 time step simulations, as shown by the purple lines[1] in Fig. 6(g)–(i). It should be noted that the overall micelle sizes are larger than those in E_4O_{11}/PPO system with $\gamma = 9{:}1$ due to different chain lengths of the polymers. The mean radius of gyration $R_g = 11.0$ nm with PPO chain length 5, $R_g = 4.9$ nm with PPO chain length 20, and $R_g = 9.2$ nm with PPO chain length 30. This result also demonstrates when the chain length of PPO is shorter or longer than that of PEE-*b*-PEO, larger multicompartment micelles are easy to be obtained.

4. Conclusions

We adopt a systematic coarse-graining strategy that several segments are coarse-grained into a single bead, and the interaction parameters between beads are estimated from the Flory–Huggins χ parameters. Our DPD results *in silico* are in agreement with those in the experiments not only on the micelle morphologies but also on the micelle sizes [7]. We then adopt the approach to study the mixing of PEE-*b*-PEO and PPO in water and try to find the conditions of forming multicompartment micelles by changing the polymer chain lengths and the volume fraction ratios between PPO and PEE-*b*-PEO. Two kinds of multicompartment micelles are obtained for the systems with small amount of PPO. The core–shell–corona micelle is observed in the condition of short chain length of PEE-*b*-PEO, whereas the micelle with two spherical compartments is formed in the condition of long chain length of PEE-*b*-PEO. These novel multicompartment micelle structures have not been observed experimentally in these diblock copolymer/homopolymer/water systems, and if experimentally verified they could provide cheaper and simpler alternatives to miktoarm star polymers. The results in

this work primarily complement the experiments with the possibilities on the preparation of multicompartment micelles using a more simple and economical approach.

Acknowledgment

This work is supported by National Science Foundation of China (20774036), the Program for New Century Excellent Talents in University of China, and Fok Ying Tung Education Foundation (114018). We thank Dr. Zhibo Li for helpful and fruitful discussion.

References

[1] Laschewsky A. Curr Opin Colloid Interface Sci 2003;8(3):274–81.
[2] Lutz JF, Laschewsky A. Macromol Chem Phys 2005;206(8):813–7.
[3] Li Z, Kesselman E, Talmon Y, Hillmyer MA, Lodge TP. Science 2004;306(5693):98–101.
[4] Lodge TP, Rasdal A, Li Z, Hillmyer MA. J Am Chem Soc 2005;127(50):17608–9.
[5] Li Z, Hillmyer MA, Lodge TP. Macromolecules 2006;39(2):765–71.
[6] Li Z, Hillmyer MA, Lodge TP. Nano Lett 2006;6(6):1245–9.
[7] Li Z, Hillmyer MA, Lodge TP. Langmuir 2006;22(22):9409–17.
[8] Liu C, Hillmyer MA, Lodge TP. Langmuir 2008;24(20):12001–9.
[9] Hillmyer MA. Science 2007;317(5838):604–5.
[10] Kotzev A, Laschewsky A, Adriaensens P, Gelan J. Macromolecules 2002;35(3):1091–101.
[11] Kubowicz S, Baussard JF, Lutz JF, Thünemann AF, Berlepsch HV, Laschewsky A. Angew Chem Int Ed 2005;44(33):5262–5.
[12] Thünemann AF, Kubowicz S, Berlepsch HV, Möhwald H. Langmuir 2006;22(6):2506–10.
[13] Kubowicz S, Thünemann AF, Weberskirch R, Möhwald H. Langmuir 2005;21(16):7214–9.
[14] Cui H, Chen Z, Zhong S, Wooley KL, Pochan DJ. Science 2007;317(5838):647–50.
[15] Mao J, Ni P, Mai Y, Yan D. Langmuir 2007;23(9):5127–34.
[16] Zhong C, Liu D. Macromol Theory Simul 2007;16(2):141–57.
[17] Xia J, Zhong C. Macromol Rapid Commun 2006;27(14):1110–4.
[18] Liu D, Zhong C. Macromol Rapid Commun 2007;28(3):292–7.
[19] Xia J, Liu D, Zhong C. Phys Chem Chem Phys 2007;9:5267–73.
[20] Liu D, Zhong C. Polymer 2008;49(5):1407–13.
[21] Huang C, Fang H, Lin C. Phys Rev E 2008;77:031804-1–8.
[22] Chou S, Tsao H, Sheng Y. J Chem Phys 2006;125(19):194903-1–6.
[23] Zhao Y, Liu Y, Lu Z, Sun C. Polymer 2008;49(22):4899–909.
[24] Hoogerbrugge PJ, Koelman JMVA. Europhys Lett 1992;19(3):155–60.
[25] Groot RD, Warren PB. J Chem Phys 1997;107(11):4423–35.
[26] Español P, Warren PB. Europhys Lett 1995;30(4):191–6.
[27] Groot RD, Madden TJ. J Chem Phys 1998;108(20):8713–24.
[28] Li Y, Hou T, Guo S, Wang K, Xu X. Phys Chem Chem Phys 2000;2:2749–53.
[29] Spyriouni T, Vergelati C. Macromolecules 2001;34(15):5306–16.
[30] Soto-Figueroa C, Rodríguez-Hidalgo M, Martínez-Magadán J. Polymer 2005;46(18):7485–93.
[31] Soto-Figueroa C, Vicente L, Martínez-Magadán J, Rodríguez-Hidalgo M. Polymer 2007;48:3902–11.
[32] Soto-Figueroa C, Vicente L, Martínez-Magadán J, Rodríguez-Hidalgo M. J Phys Chem B 2007;111:11756–64.
[33] Soto-Figueroa C, Rodríguez-Hidalgo M, Martínez-Magadán J, Vicente L. Macromolecules 2008;41:3297–304.
[34] Ortiz V, Nielsen SO, Discher DE, Klein ML, Lipowsky R, Shillcock J. J Phys Chem B 2005;109(37):17708–14.
[35] Groot RD, Rabone KL. Biophys J 2001;81(2):725–36.
[36] Guo SL, Hou TJ, Xu XJ. J Phys Chem B 2002;106(43):11397–403.
[37] van Vlimmeren BAC, Maurits NM, Zvelindovsky AV, Sevink GJA, Fraaije JGEM. Macromolecules 1999;32(3):646–56.
[38] Fraaije JGEM, Sevink GJA. Macromolecules 2003;36(21):7891–3.
[39] Maiti A, McGrother S. J Chem Phys 2004;120(3):1594–601.
[40] Lee W, Ju S, Wang Y, Chang J. J Chem Phys 2007;127(6):064902.
[41] Sun H. J Phys Chem B 1998;102(38):7338–64.
[42] Sun H, Ren P, Fried JR. Comput Theor Polym Sci 1998;8(1–2):229–46.
[43] Rigby D, Sun H, Eichinger BE. Polym Int 1997;44(3):311–30.
[44] Allen MP, Tildesley DJ. Computer simulation of liquids. Oxford: Clarendon Press; 1987.
[45] Wang XL, Lu ZY, Li ZS, Sun CC. J Phys Chem B 2005;109(37):17644–8.
[46] Berendsen HJC, Postma JPM, van Gunsteren WF, DiNola A, Haak JR. J Chem Phys 1984;81(8):3684–90.
[47] Li Z, Lu Z, Sun Z, Li Z, An L. J Phys Chem B 2007;111(21):5934–40.
[48] Özen AS, Sen U, Atilgan C. J Chem Phys 2006;124:064905-1–9.
[49] Boryczko K, Dzwinel W, Yuen DA. Concurrency Computat Pract Exper 2002;14:137–61.
[50] Sims JS, Martys N. J Res Natl Inst Stand Technol 2004;109(2):267–77.
[51] Zhao Y, Liu H, Lu ZY, Sun CC. Chin J Chem Phys 2008;21(5):451–6.
[52] Sheng Y, Wang T, Chen WM, Tsao H. J Phys Chem B 2007;111(37):10938–45.
[53] Scocchi G, Posocco P, Fermeglia M, Pricl S. J Phys Chem B 2007;111(9):2143–51.